Acta Polytechnica CTU Proceedings **56**:41–45, 2026
https://doi.org/10.14311/APP.2026.56.0041

Published by the Czech Technical University in Prague

DERIVATION OF SOIL SHEAR MODULUS FROM PUSH AND PULL TESTS OF MICROPILES

Karel Vojtasík

VSB - Technical University of Ostrava, Department of Geotechnics and Underground Engineering, Ludvíka Podéště 1875/17, 708 00 Ostrava – Poruba, Czech Republic

correspondence: karel.vojtasik@vsb.cz

Abstract. The article presents a method for earning soil shear modules from the results of micropile loading tests. The micropile is first loaded with a push force and then with a pull force. The shear modules are derived from two graphs of the dependence of micropile displacements on the loading forces. One represents a push and the other a pull test. Three values of soil shear moduli are obtained, namely for elastic deformation, plastic hardening and the last one after soil failure at a slip plane on micropile shaft.

Keywords: Soil, shear module, micropile, load test.

1. Introduction

The stiffness of soil is typically determined by its strain, with its behaviour being considered elastoplastic. Numerous authors have investigated this dependency through laboratory tests, including Duncan and Chang [1], Burland [2], and LoPresti et al. [3]. The shear modulus G has been determined by measuring the propagation velocity of the shear wave in loaded soil samples. This dependency results in an uneven decrease of the soil's shear stiffness during deformation, as noted by Atkinson and Sallfors [4]. Hardin and Drnevich [5], as well as Fahey and Carter [6], have proposed an analytical expression for the decrease in shear soil stiffness due to deformation, utilizing a hyperbolic dependency that associates shear modulus with shear deformation. The elastoplastic behaviour of soil can be described in three phases: first, at the consolidated state of the soil, the behaviour is elastic for a small strain with a high shear modulus G_e. This is followed by a plastic phase during hardening of the soil, with a noticeably lower shear modulus G_h and a wider range of deformation involving rotational and laminar rearrangement of soil particles. The final phase involves a continuation strain and represents the existence of a shear plane in the soil with a residual shear modulus G_r.

2. Function and load tests of micropile

Micropiles that are installed solely in soil and not leaning on hard subgrade serve to transfer axial force into the soil through shear stress on the micropile shaft. Due to its significantly higher stiffness compared to soil, the micropile displacement only results from the shear strain of the soil at the interface. The loaded micropile slides uniformly in the soil, inducing uniform shear stress at the interface along the entire shaft length and perimeter. The micropile's function in soil

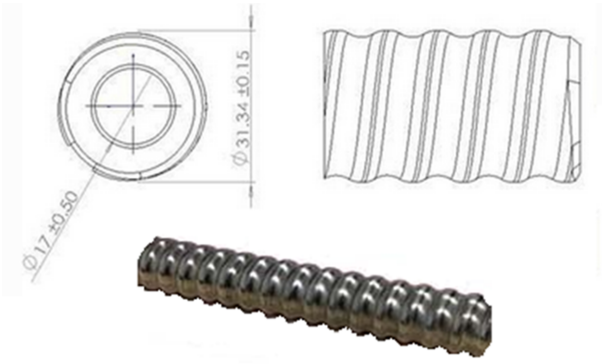

Figure 1. Micropile from hollow steel rod type R32.

establishes a relationship between displacement and load force, which inherently includes all design and soil parameters. This relationship can be experimentally determined through push and pull force loading and analysed through dependence curves from measured displacements and forces for each type of loading.

Four identical micropiles were installed on monotonous soil consisting only of loess clays. The micropile consists of a hollow steel rod with a corrugated surface, type R32 (see Figure 1). The rod is 3 m long and at the toe, it is equipped with a drill bit of 45 mm diameter. The micropile was manually installed by rotary percussion drilling and grouted with epoxy resin from the toe.

The four micropiles were installed on the same ground profile. The topsoil of 0.8 m from anthropogenic sediments and soil with organic content was replaced with compacted clayey sand and the rest of the profile consisted of loess clay to a depth of approximately 5.5 m, the parameters of which are given in Table 1. The micropile is first pushed until the transmitted push force significantly drops at large displacements. Thereafter the micropile is pulled out while the transmitted pulling force increases until it

Depth [m]	2	2.7
Density [g cm^{-3}]	19.8	20.7
Porosity [%]	40	39
Water content [%]	19.8	20.7
Liquid limit [%]	31.5	36.9
Plastic limit [%]	16.5	16.0
Saturation degree	0.8	0.87
Effective cohesion [kPa]	8	8
Effective angle of friction [°]	25	25
E modulus [kPa]	–	6 900

Table 1. Loess clay parameters.

stabilizes. The pull test is finished at a displacement of 25 mm. Between the two tests, there is a time delay of about a week, which is needed to remove the concrete cube foot from the micropile head. The dimensions of the concrete cubic foot are 400 × 400 × 300 mm. Its role consists of several functions. The chief one is to eliminate the effect of eccentricity from applied push force because this could bring about deflection of the upper section of the micropile rod and in this way significantly distort the value of displacements. The next one is to enable the installation of a hydraulic press and so to create a base for four transducers placed at each corner of the foot to read the displacements.

The dependence curve of displacement on force obtained for the micropile with concrete cube foot incorporates an effect of the concrete cube foot also. Elimination of the influence from the dependence curve is accomplished simply by subtracting a dependence curve of displacement on force for a concrete cube foot without micropile from the dependence curve of displacement on force with a concrete cube foot. Therefore, a compressive load test was carried out for the concrete cube foot at the same soil ground profile. The micropile loading in both tests progressed in loading steps with a force increase of 10 kN in the push test and 5 kN in the pull test. Each increase in loading force was followed by a waiting period until the micropile movement was stopped. During the micropile moving in waiting time, the force increment dropped a bit as the hydraulic press did not maintain a respective force. Once a micropile movement ceased, displacement and force values were recorded. In the respective loading steps, a 10-minute waiting time was sufficient to stop the movement of the micropiles. The load tests were always terminated when the total displacement of the micropile exceeded 25 mm in both tests. After the pull test, the micropile was removed from the soil, measured its diameter and evaluated the state of the column surface of the micropile (see Figure 2). The steel rods of all four micropiles were surrounded along their entire length by a ring of injected soil, which was glued to the steel rods. The diameters of the micropiles columns extracted from the soil along their length ranged from 60 to 75 mm.

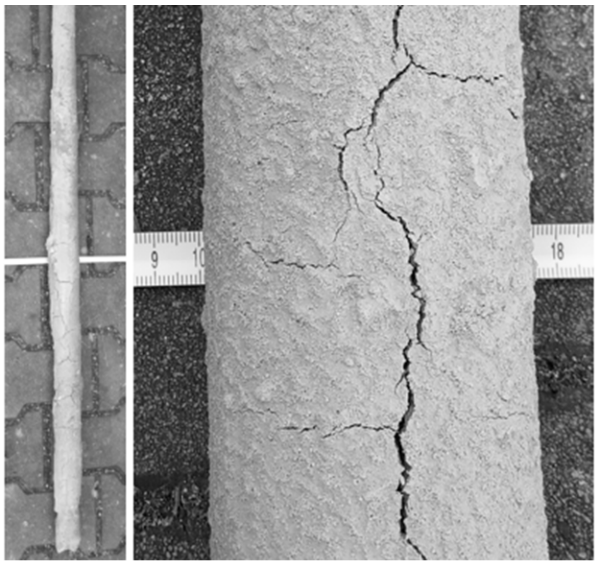

Figure 2. Micropile after extraction from the ground after test.

3. Analysis

The method is based on the following assumptions:

- elastic-plastic behaviour of soil,
- there is considered only deformation of the softest compound represented here by the thin soil layer on the perimeter of the micropile shaft,
- the displacement of the micropile u is equated with shear strain $\gamma (u \to \gamma)$,
- uniform distribution of shear stress on the perimeter and along the micropile shaft,
- volumetric strain on the soil on the perimeter of the micropile shaft is not included in the analysis,
- shear strain modules are the secant lines of the dependence curve of displacement on shear stress,
- known design parameters of the micropile (length, diameter of the shaft),
- analysis is performed on two shear stress displacement curves, one for the push test and the other for the pull test, both of which generalize the behaviour of four real micropiles and their shear stress displacement curves obtained by measurement. Their derivation is not included in this article, and it is documented in detail in the research reports 'Vojtasik [7, 8]' and supplementary materials.

The shear stress values at the micropile shaft τ are calculated according to the formula.

$$\tau = F/A, \tag{1}$$

where F – micropile load force [kN], A – area of the micropile shaft [m^2].

$$A = \pi \cdot D \cdot l, \tag{2}$$

where D – diameter of micropile shaft [m], l – micropile length [m].

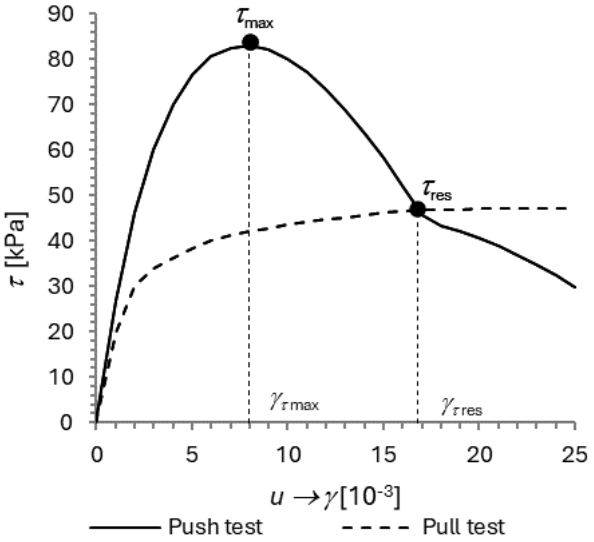

FIGURE 3. Graphs of dependence of shear stress on deformation extracted from push and pull tests.

Figure 3 shows the dependence curves of the displacement u on shear stress τ at micropile shaft from the push and pull tests for the micropiles, which have a length of $l = 3\,\mathrm{m}$ and a diameter of the micropile shaft considered of $D = 75\,\mathrm{mm}$ (see Figure 2).

The modulus of deformation of an elastic-plastic material depends on the deformation and so does the shear modulus of the soil in proximity to the micropile shaft. The shear strain behaviour during the push test will be elastic at the beginning. After some deformation, the elastic behaviour becomes plastic with the maximum value of τ_{max} at the respective micropile displacement u_{max}. Then, with further micropile displacement the shear stress drops. The maximum shear stress τ_{max} splits the course of the plastic straining into two soil states. The first stands for elastoplastic deformation, and the second stands for the initialisation of the formation of a slip plane with its full development at the residual shear stress τ_{res}. Thus, on the curve for the push test in Figure 3 we can differentiate three stretches representing each of them with a particular shear strain modulus. The first elastic modulus is G_e, the second strain hardening modulus G_h, and the third residual modulus G_r for the resulting slip plane. The shear strain modules G_e and G_h are derived from the courses of dependence curves of displacement u on shear stress τ of both types of tests under the application of two presumptions. It is assumed that the courses of plastic behaviour during strain hardening are identical for both types of tests. Thus, the increase in plastic strain for hardening $\Delta\gamma_h$ in both curves will be of the same magnitude, and therefore the shear strain modules for hardening G_h derived from the curves of dependence of displacement u on shear stress τ must be of the same magnitude also (see Figure 4a). The other expects that the elastic modulus G_e has the same magnitude as in both dependency curves but the magnitudes of elastic strain of

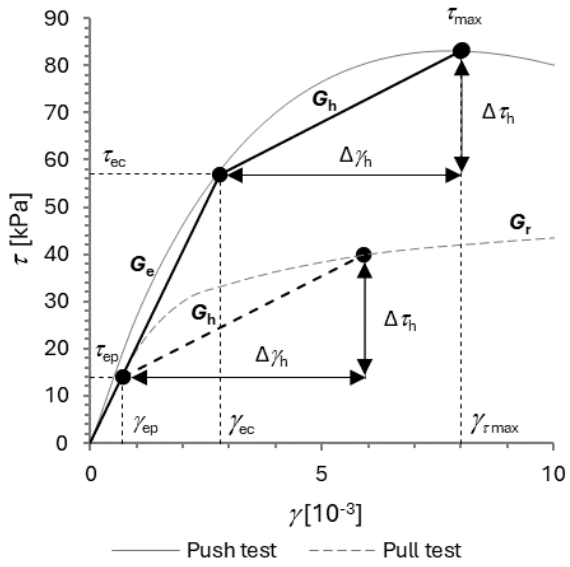

(A).

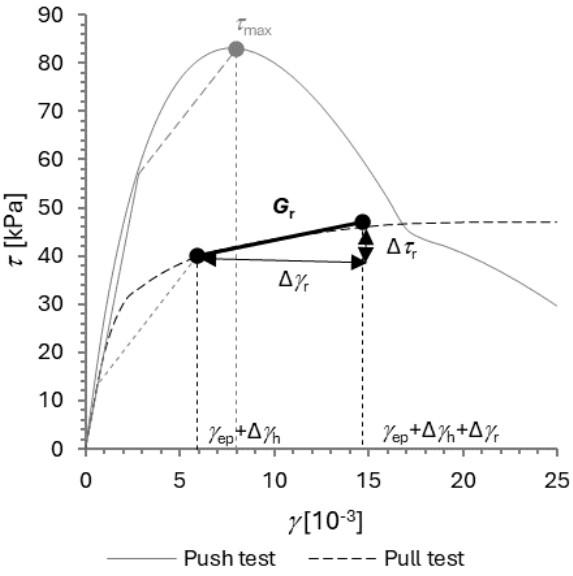

(B).

FIGURE 4. Graphical representations of modules G_e, G_h and G_r.

push test $\Delta\gamma_{ec}$ and pull test $\Delta\gamma_{ep}$ are different. This difference is due to sequence of push and pull tests. The push test was performed first on consolidated soil while the next pull test after on soil already in a plastic state. The effect of elastic strain is minimal in the pull test, whereas the hardening effect manifests itself in the same range of strain as in the push test because the micropile has moved in the opposite direction in the pull test as that in the push test. Under the above-mentioned assumptions, it is possible experimentally to assign unambiguously sections on both curves to the relevant shear deformation modules.

A practical implementation for meeting the above assumptions consists of searching for the position of γ_e, τ_e, on the strain-stress graph of the compressive

test until these assumptions are met. The magnitudes of the respective shear modules are given by formulas.

$$G_e = \frac{\tau_{ec}}{\gamma_{ec}}, \tag{3}$$

$$G_h = \frac{(\tau_{max} - \tau_{ec})}{(\gamma_{\tau max} - \gamma_{ec})} = \frac{\Delta\tau_h}{\Delta\gamma_h}. \tag{4}$$

The shear modulus G_r is derived using the same assumption as for G_r and that the respective increment of strain $\Delta\gamma_r$ to calculate this modulus must be of the same magnitude in the curves of dependence of the displacement u on shear stress τ of both types of tests. The strain increment $\Delta\gamma_r$ is equal to

$$\Delta\gamma_r = \gamma_{\tau res} - \gamma_{\tau max}. \tag{5}$$

The scheme for enumeration of the strain modulus G_r is derived from the curve of dependence of displacement u on shear stress τ for pull test as is documented in Figure 4b. The magnitude of the shear strain module for softening G_r is given by formula.

$$G_r = \frac{\tau_{res} - (\tau_{ep} - \Delta\tau_h)}{(\gamma_{\tau res} - \gamma_{\tau max})} = \frac{\Delta\tau_r}{\Delta\gamma_r}. \tag{6}$$

4. Calculation of modules

The values of input parameters τ_{max} and $u_{\tau max}$ for calculation of modules G_e and G_h given by formulae (3) and (4) are read out from the respective strain-stress graphs in Figure 3.

$$\tau_{max} = 83\,\text{kPa}$$
$$\gamma_{\tau max} = 0.008$$

The values of γ_e, τ_e on the strain-stress curve for the push test are determined by random selection until secants for G_h on the both strain-stress curves attained the identical value and while the strain-stress curve for the pull test gets through γ_h, τ_h.

$$\gamma_{ec} = 0.0028$$
$$\tau_{ec} = 57\,\text{kPa}$$
$$G_e = \frac{57}{0.0028} \approx 20\,400\,\text{kPa}$$

The modulus G_h is calculated by formulae (4)

$$\Delta\gamma_h = \gamma_{\tau max} - \gamma_{ec} = 0.008 - 0.0028 = 0.0052$$
$$\Delta\tau_h = \tau_{max} - \tau_{ec} = 83 - 57 = 26\,\text{kPa}$$
$$G_h = \frac{26}{0.0052} = 5\,000\,\text{kPa}$$

The values of parameters τ_{ep}, $\gamma_{\tau res}$ and τ_{res} for calculation of modulus G_r given by formulae (6) are taken from the respective strain-stress graphs in Figures 3 and 4.

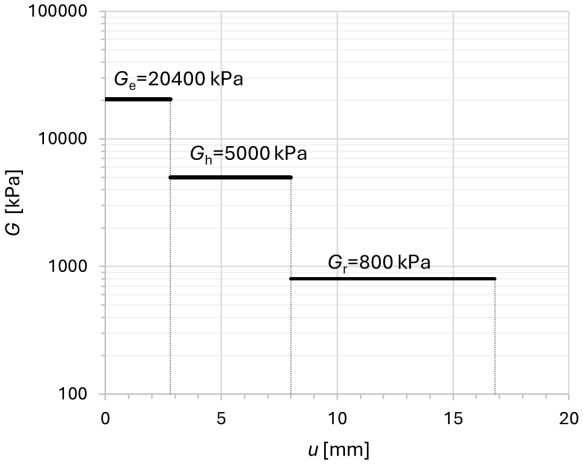

Figure 5. The values of the modules G_e, G_h and G_r relative to the displacement of the micropile u.

$$\tau_{ep} = 14\,\text{kPa}$$
$$\gamma_{\tau res} = 0.0168$$
$$\tau_{res} = 47\,\text{kPa}$$
$$\Delta\tau_r = \tau_{res} - (\tau_{ep} + \Delta\tau_h) = 47 - (14 + 26) = 7\,\text{kPa}$$
$$\Delta\gamma_r = \gamma_{\tau res} - \gamma_{\tau max} = 0.0168 - 0.008 = 0.0088$$
$$G_r = \frac{7}{0.0088} \approx 800\,\text{kPa}$$

Figure 5 shows the dependence of the modulus value on the displacement of the micropile.

5. Discussion

The derivation of the modules G_h and G_r comes from the the assumption that the range values of $\Delta\gamma_h$ or $\Delta\gamma_r$ is independent on tests to establish them either by the push test or the pull test. The assumption about $\Delta\gamma_h$ allows us to find out its magnitude from the shear stress displacement curves for the push and pull tests because on both curves there can be found sections with nearly identical deformational development (see Figure 6).

The apparent four-fold difference in the magnitudes of the elastic strain in the push test (2.8 mm) and the pull test (0.7 mm) is the consequence that the pull test was performed with a predisposition of the slip plane in the soil near the micropile shaft. After a short elastic deformation, the strain hardening followed due to the opposite direction of the micropile movement during the pull test. The determined magnitudes of the shear strain modules G_e, G_h and G_r at micropile shaft do not contradict the generally known fact that the magnitudes of the strain modulus are dependent on the strain and decrease with increasing strain. The G_h value of 5 000 kPa determined by this

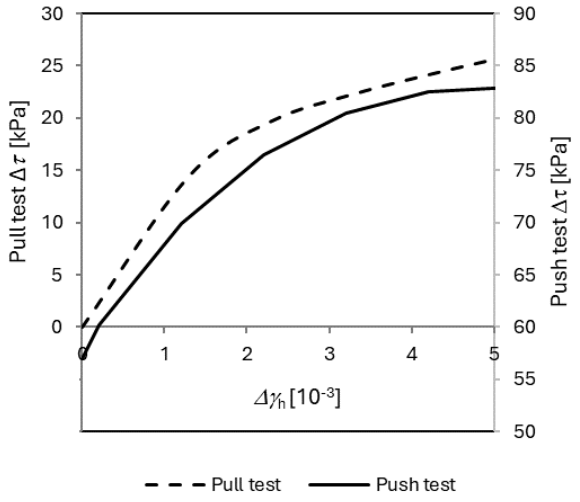

FIGURE 6. The graphs of the stress-strain dependence in the soil hardening stage.

presented method is approximately twice the G value of 2 654 kPa, which is derived from the modulus E of 6 900 kPa (see Table 1) and the Poisson number of 0.3 was chosen to convert the value of E to G. The reasons for the different modules can be seen in the testing boundary conditions. In the micropile test, they are implicitly present here. In the laboratory, the test conditions are set, and the setting may not fully correspond to those in the real site. In a laboratory test, the structure of a soil sample is usually disturbed during sample collection and handling. These circumstances can explain the difference in the module values. Therefore, the module from the micropile tests can be more dependable than the one from the laboratory test. From another point of view, none of the given G_h or G values is outside the range of common values for soils.

6. Conclusions

The presented methodology shows a way to determine the dependence of the shear modules on soil deformation using a simple force approach from the dependence curves of displacement u on shear stress τ.

The methodology does not include the usual disturbing circumstances that accompany the preparation and performance of laboratory tests on collected soil samples and that distort the results.

The advantage of the methodology is that it implicitly and comprehensively includes intrinsic soil ground phenomena in the tested area, which cannot be generally implemented in laboratory tests.

The known shear modules G_e and G_h enable one to assess the bearing capacity of the micropile from its settlement, which is a decisive parameter of its application in practical tasks and is required by standards and regulations for their application. The value of moduli G_r completes the range of values of shear deformation soil modules and can be used to evaluate for task of soils large deformations.

Acknowledgements

This contribution was made as part of the conceptual development of science, research, and innovations in 2019 and 2020, which was supported by VŠB-Technical University in Ostrava, Faculty of Civil Engineering.

References

[1] J. M. Duncan, Y. Chang. Nonlinear analysis of stress and strain in soils. In *ASCE*, vol. 96, pp. 1629–1654. 1970.

[2] J. B. Burland. Ninth Laurits Bjerrum memorial lecture: "Small is beautiful" – the stiffness of soils at small strains. *Canadian Geotechnical Journal* **26**(4):499–516, 1989. https://doi.org/10.1139/t89-064

[3] D. C. F. Lo Presti, O. Pallara, R. Lancellotta, et al. Monotonic and cyclic loading behavior of two sands at small strains. *Geotechnical Testing Journal* **16**(4):409–424, 1993. https://doi.org/10.1520/GTJ10281J

[4] J. H. Atkinson, G. Sallfors. Experimental determination of soil properties. In *Proceedings of the 10th ECSMFE*, vol. 3, pp. 915–956. 1991.

[5] B. O. Hardin, V. P. Drnevich. Shear modulus and damping in soils: Design equations and curves. *Journal of the Soil Mechanics and Foundations Division* **98**(7):667–692, 1972. https://doi.org/10.1061/JSFEAQ.0001760

[6] M. Fahey, J. P. Carter. A finite element study of the pressuremeter test in sand using a nonlinear elastic plastic model. *Canadian Geotechnical Journal* **30**(2):348–362, 1993. https://doi.org/10.1139/t93-029

[7] K. Vojtasik. Determination of micropile bearing capacity in soil underneath an experimental frame, 2019. Research Report No. IP2249931; VSB – Technical University of Ostrava, Department of Geotechnics and Underground Engineering.

[8] K. Vojtasik. Determination of strength and deformation parameters of micropile-interface by a simultaneous numerical and experimental approach, 2020. Research Report No. IP2240051; VSB – Technical University of Ostrava, Department of Geotechnics and Underground Engineering.